



How Much More Rain Will Global Warming Bring?

Frank J. Wentz, *et al.*
Science **317**, 233 (2007);
DOI: 10.1126/science.1140746

The following resources related to this article are available online at www.sciencemag.org (this information is current as of July 27, 2007):

Updated information and services, including high-resolution figures, can be found in the online version of this article at:

<http://www.sciencemag.org/cgi/content/full/317/5835/233>

Supporting Online Material can be found at:

<http://www.sciencemag.org/cgi/content/full/1140746/DC1>

This article **cites 14 articles**, 2 of which can be accessed for free:

<http://www.sciencemag.org/cgi/content/full/317/5835/233#otherarticles>

This article appears in the following **subject collections**:

Atmospheric Science

<http://www.sciencemag.org/cgi/collection/atmos>

Information about obtaining **reprints** of this article or about obtaining **permission to reproduce this article** in whole or in part can be found at:

<http://www.sciencemag.org/about/permissions.dtl>

15. T. Kunihiro, K. Nagashima, H. Yurimoto, *Geochim. Cosmochim. Acta* **69**, 763 (2005).
16. Materials and methods are available as supporting material on Science Online.
17. K. Nagashima, A. N. Krot, H. Yurimoto, *Nature* **428**, 921 (2004).
18. E. D. Young, S. S. Russell, *Science* **282**, 452 (1998).
19. $\delta^{18}\text{O}_{\text{SMOW}} (\text{‰}) \equiv [(^{18}\text{O}/^{16}\text{O})_{\text{sample}} / (^{18}\text{O}/^{16}\text{O})_{\text{SMOW}} - 1] \times 1000$, where $i = 17$ or 18.
20. T. R. Ireland, P. Holden, M. D. Norman, J. Clarke, *Nature* **440**, 776 (2006).
21. L. H. Fuchs, E. Olsen, K. J. Jensen, *Smithson. Contrib. Earth Sci.* **10**, 1 (1973).
22. K. Tomeoka, P. R. Buseck, *Geochim. Cosmochim. Acta* **49**, 2149 (1985).
23. B. Fegley Jr., *Space Sci. Rev.* **92**, 177 (2000).
24. D. S. Lauretta, D. T. Kremser, B. Fegley Jr., *Icarus* **122**, 288 (1996).
25. Y. Hong, B. Fegley Jr., *Meteorit. Planet. Sci.* **33**, 1101 (1997).
26. R. N. Clayton, T. K. Mayeda, *Geochim. Cosmochim. Acta* **63**, 2089 (1999).
27. A. Greshake, *Geochim. Cosmochim. Acta* **61**, 437 (1997).
28. E. D. Young, *Philos. Trans. R. Soc. London A* **359**, 2095 (2001).
29. B.-G. Choi, K. D. McKeegan, A. N. Krot, J. T. Wasson, *Nature* **392**, 577 (1998).
30. A. N. Krot, B. Fegley Jr., K. Lodders, H. Palme, in *Protostars and Planets IV*, V. Mannings, A. P. Boss, S. S. Russell, Eds. (Univ. of Arizona Press, Tucson, AZ, 2000) pp. 1019–1054.
31. J. M. W. Chase, *NIST-JANAF Thermochemical Tables, Fourth edition, Journal of Physical and Chemical Reference Data, Monograph 9, Parts I and II* (American Institute of Physics, New York, 1998).
32. We thank Y. Matsuhsa for providing a magnetite standard, T. Kaito and I. Nakatani for assistance with focused ion beam sample preparation, K. Tomeoka for indicating Murchison tochilinite, and E. D. Scott and G. R. Huss for discussion. This work was partly supported by Monkasho (H.Y.) and NASA (A.N.K.).

Supporting Online Material

www.sciencemag.org/cgi/content/full/1142021/DC1
Materials and Methods
Fig. S1
Tables S1 and S2
References

2 March 2007; accepted 17 May 2007
Published online 14 June 2007;
10.1126/science.1142021
Include this information when citing this paper.

How Much More Rain Will Global Warming Bring?

Frank J. Wentz,* Lucrezia Ricciardulli, Kyle Hilburn, Carl Mears

Climate models and satellite observations both indicate that the total amount of water in the atmosphere will increase at a rate of 7% per kelvin of surface warming. However, the climate models predict that global precipitation will increase at a much slower rate of 1 to 3% per kelvin. A recent analysis of satellite observations does not support this prediction of a muted response of precipitation to global warming. Rather, the observations suggest that precipitation and total atmospheric water have increased at about the same rate over the past two decades.

In addition to warming Earth's surface and lower troposphere, the increase in greenhouse gas (GHG) concentrations is likely to alter the planet's hydrologic cycle (1–3). If the changes in the intensity and spatial distribution of rainfall are substantial, they may pose one of the most serious risks associated with climate change. The response of the hydrologic cycle to global warming depends to a large degree on the way in which the enhanced GHGs alter the radiation balance in the troposphere. As GHG concentrations increase, the climate models predict an enhanced radiative cooling that is balanced by an increase in latent heat from precipitation (1, 2). The Coupled Model Intercomparison Project (4) and similar modeling analyses (1–3) predict a relatively small increase in precipitation (and likewise in evaporation) at a rate of about 1 to 3% K^{-1} of surface warming. In contrast, both climate models and observations indicate that the total water vapor in the atmosphere increases by about 7% K^{-1} (1–3, 5, 6).

More than 99% of the total moisture in the atmosphere is in the form of water vapor. The large increase in water is due to the warmer air being able to hold more water vapor, as dictated by the Clausius-Clapeyron (C-C) relation under the condition that the relative humidity in the lower troposphere stays constant. So according

to the current set of global coupled ocean-atmosphere models (GCMs), the rate of increase in precipitation will be several times lower than that for total water. This apparent inconsistency is resolved in the models by a reduction in the vapor mass flux, particularly with respect to the Walker circulation, which reinforces the trade winds (3, 7). Whether a decrease in global winds is a necessary consequence of global warming is a complex question that is yet to be resolved (8).

Using satellite observations from the Special Sensor Microwave Imager (SSM/I), we assessed the GCMs' prediction of a muted response of rainfall and evaporation to global warming. The SSM/I is well suited for studying the global hydrologic cycle in that it simultaneously measures precipitation (P), total water vapor (V), and also surface-wind stress (τ_0), which is the principal term in the computation of evaporation (E) (8, 9).

The SSM/I data set extends from 1987 to 2006. During this time Earth's surface temperature warmed by $0.19 \pm 0.04 \text{ K decade}^{-1}$, according to the Global Historical Climatology Network (10, 11). Satellite measurements of the lower troposphere show a similar warming of $0.20 \pm 0.10 \text{ K decade}^{-1}$ (12). The error bars are at the 95% confidence level. This warming is consistent with 20th-century climate-model runs (13) and provides a reasonable, albeit short, test bed for assessing the impact of global warming on the hydrologic cycle.

When averaged globally over monthly time scales, P and E must balance except for a

negligibly small storage term. This $E = P$ constraint provides a useful consistency check with which to evaluate our results. However, the constraint is valid only for global averages. Accordingly, the first step in our analysis was to construct global monthly maps of P and E at a 2.5° spatial resolution for the period 1987 to 2006.

The SSM/I retrievals used here are available only over the ocean. To supplement the SSM/I over-ocean rain retrievals, we used the land values from the Global Precipitation Climatology Project data set, which is a blend of satellite retrievals and rain gauge measurements (14, 15). Satellite rain retrievals over land were less accurate than their ocean counterparts, but this drawback was compensated by the fact that there are abundant rain gauges over land for constraining the satellite retrievals. Likewise, global evaporation was computed separately for oceans and land. Because 86% of the world's evaporation comes from the oceans (16), ocean evaporation was our primary focus. We computed evaporation over the oceans with the use of the bulk formula from the National Center for Atmospheric Research Community Atmospheric Model 3.0 (8, 17). Evaporation over land cannot be derived from satellite observations, and we resorted to using a constant value of 527 mm year^{-1} for all of the continents, excluding Antarctica (16). For Antarctica and sea ice, we used a value of 28 mm year^{-1} (8, 16).

The GCMs indicate that E should increase about 1 to 3% K^{-1} of surface warming. However, according to the bulk formula (eq. S1) (8), evaporation increases similarly to C-C as the surface temperature warms, assuming that the other terms remain constant. For example, a global increase of 1 K in the surface air temperature produces a 5.7% increase in E (8). To obtain the muted response of 1 to 3% K^{-1} , other variables in the bulk formula need to change with time. The air-sea temperature difference and the near-surface relative humidity are expected to remain nearly constant (8), and this leaves τ_0 as the one variable that can reduce evaporation to the magnitude required to balance the radiation budget in the models. To bring the bulk formula into agreement with the radiative cooling constraint, $\sqrt{\tau_0}$

Remote Sensing Systems, 438 First Street, Santa Rosa, CA 95401, USA.

*To whom correspondence should be addressed. E-mail: frank.wentz@remss.com

would need to decrease by about $4\% \text{ K}^{-1}$. Thus, a muted response of precipitation to global warming requires a decrease in global winds (2, 3, 7).

To evaluate the GCMs' prediction of a decrease in winds, we looked at the 19 years of SSM/I wind retrievals. These winds are expressed in terms of an equivalent neutral-stability wind speed (W) at a 10-m elevation, which is proportional to $\sqrt{v_0}$ (8, 16). Figure 1 shows a decadal trend map of W . For each 2.5° grid cell, a least-squares linear fit to the 19-year time series was calculated after removing the seasonal variability. The wind trends from the International Comprehensive Ocean-Atmosphere Data Set (ICOADS) are also shown, but just for comparison. They were not used in our analysis. Although the ICOADS trend map is very noisy because of sampling and measurement deficiencies, it shows trends similar to those from the SSM/I in the northern Atlantic and Pacific, where the ICOADS ship observations are more abundant. The North Atlantic Oscillation (NAO) is apparent in both trend maps as a tripole feature with increasing winds between 30°N and 40°N and decreasing winds to the north and south (18). This feature is consistent with the observed decrease in the NAO index since 1987. When averaged over the tropics from 30°S to 30°N , the winds increased by 0.04 m s^{-1} (0.6%) decade^{-1} , and over all oceans the increase was 0.08 m s^{-1} (1.0%) decade^{-1} . The SSM/I wind retrievals were validated by comparisons with moored ocean buoys and satellite scatterometer wind retrievals (fig. S1). On the basis of this analysis, the error bar on the SSM/I wind trend is estimated to be $\pm 0.05 \text{ m s}^{-1} \text{ decade}^{-1}$ at the 95% confidence level (8). This observed increase in the SSM/I winds is opposite to the GCM results, which predict that the 1987-to-2006 warming should have been accompanied by a decrease in winds on the order of $(0.19 \text{ K decade}^{-1})(4\% \text{ K}^{-1}) = 0.8\% \text{ decade}^{-1}$.

We then looked at the variability of global precipitation and evaporation during the past two decades. Figure 2A shows the time series for P and E . Also shown is the over-ocean SSM/I retrieval of V . To generate the time series, the seasonal variability was first removed, and then the variables were low-pass filtered by convolution with a Gaussian distribution that had a ± 4 -month width at half-peak power. The major features apparent in the time series are the 1997–1998 El Niño and the 1986–1987 El Niño, followed by the strong 1988–1989 La Niña. It is noteworthy that E , P , and V all exhibited similar magnitudes for interannual variability and decadal trends (Table 1). After applying the ± 4 -month smoothing, the correlation of E versus P was 0.68. Because global precipitation and evaporation must balance, the observed differences in the derived values of P and E provided an error estimate that we used to estimate the uncertainty in the decadal trend. The estimated error bar at the 95% confidence level for E and P is $\pm 0.5\% \text{ decade}^{-1}$ (8).

Also shown in Fig. 2A is the ensemble mean of nine climate-model simulations smoothed in

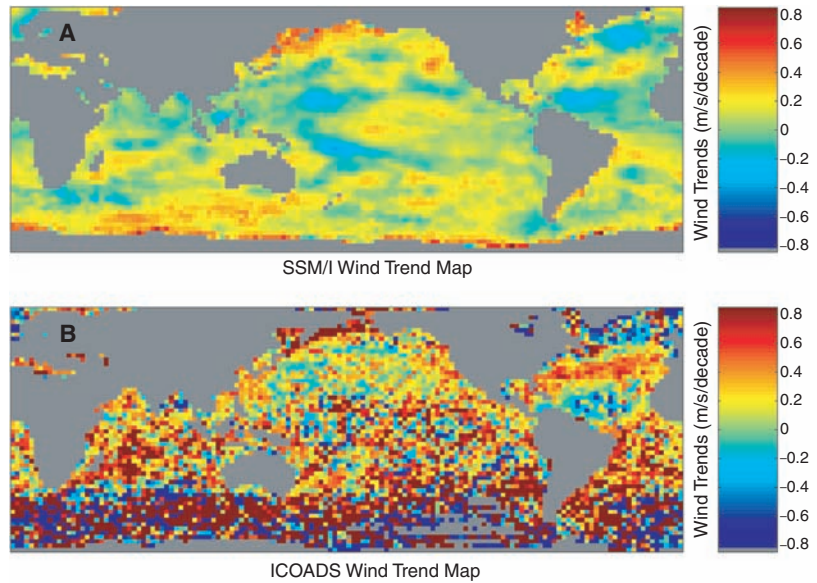


Fig. 1. Surface-wind trends for the period July 1987 through August 2006 computed at a spatial resolution of 2.5° . (A) SSM/I wind trends. (B) ICOADS wind trends. In the North Pacific and North Atlantic where ICOADS ship observations are more abundant, the two data sets show similar trends. The tripole feature in the North Atlantic is consistent with the recent decrease in the NAO index.

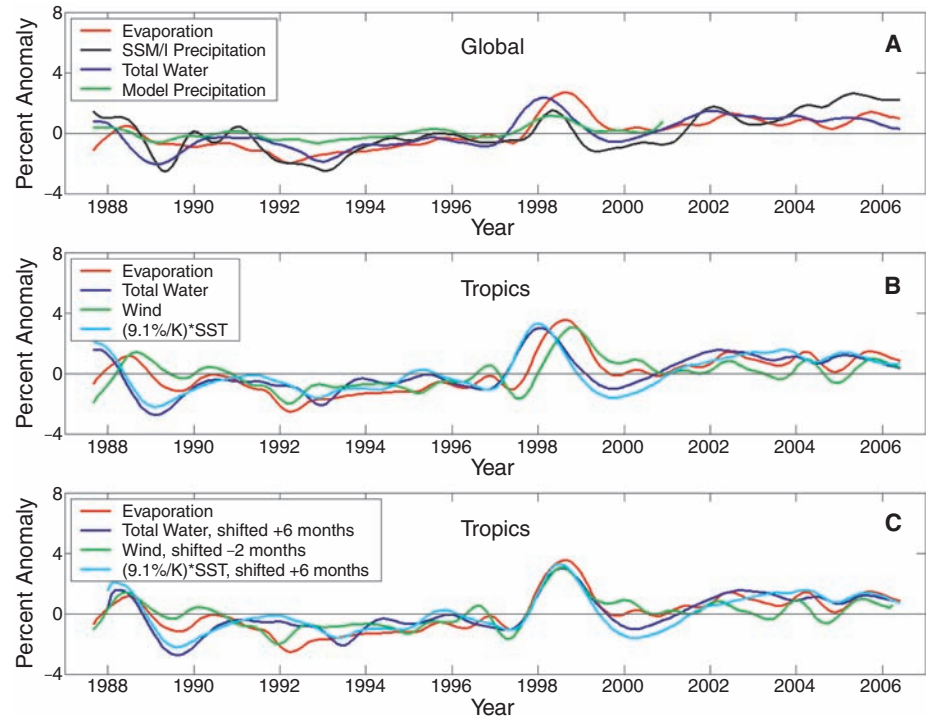


Fig. 2. Anomaly time series of the hydrologic variables. (A) Global results for the observed precipitation and evaporation and over-ocean results for total water vapor. The average model precipitation predicted by AMIP simulations is also shown. (B) Tropical ocean results for evaporation, total water vapor, surface-wind speed, and SST. The SST time series has been scaled by $9.1\% \text{ K}^{-1}$. During the El Niños, evaporation and wind were not in phase with vapor and SST. At the end of 1996, SST and vapor began to increase while the winds began to decrease, with no net effect on evaporation. About 8 months later (mid-1997), the winds in the tropics began to recover and then increased sharply, reaching a maximum value in late 1998. All four variables remained at elevated values thereafter. (C) Same as (B), except that the water vapor and SST curves have been shifted forward in time by 6 months, and the wind curve has been shifted backward by 2 months. The statistics on the global time series, including error bars, are given in Table 1.

the same way as in the satellite observations. These climate runs, for which the sea-surface temperature (SST) is prescribed from observations, are from the Atmospheric Model Intercomparison Project II (AMIP-II) (19, 20). There is a pronounced difference between the precipitation time series from the climate models and that from the satellite observations. The amplitude of the interannual variability, the response to the El Niños, and the decadal trends are all smaller by a factor of 2 to 3 in the climate-model results, as compared with the observations. This characteristic of the models to underpredict the amplitude of precipitation changes to El Niño–Southern Oscillation events has been reported previously (21), and the results presented here suggest that the climate models are also underestimating the decadal variability.

The similarity in the satellite-derived time series became more pronounced when the analysis was limited to the tropical oceans (30°S to 30°N), where most of the evaporation occurs. Although the condition $E = P$ was no longer valid for this regional analysis, the coupling of evaporation with the other variables was more apparent. Figure 2B shows the tropical time series of E , V , SST , and W . The variables V and SST exhibited a high correlation [correlation coefficient (r) = 0.96], and their scaling relation of $9.1\% \text{ K}^{-1}$ was equal to the C-C rate ($6.5\% \text{ K}^{-1}$) times a moist adiabatic lapse rate (MALR) factor of 1.4 (5). The MALR factor is the ratio of change in the lower tropospheric temperature to the change in SST . This strong coupling between V and SST is another confirmation that the total atmospheric water increases with temperature at the C-C rate.

During the two El Niños, evaporation and wind speed were not in phase with vapor and SST . The increase in evaporation lagged the in-

crease in vapor by 6 months, and the increase in winds lagged by 8 months (Fig. 2B). When a 6-month lag was applied, the correlation between E and V was 0.84 in the tropics and 0.88 globally.

Figure 3 shows a trend map of $P - E$. The most striking feature is in the tropical Western Pacific Warm Pool, where $\Delta(P - E)$ is about $400 \text{ mm year}^{-1} \text{ decade}^{-1}$, and Δ represents change. This is a region of maximum $P - E$ (1500 to $2000 \text{ mm year}^{-1}$). Simple hydrologic models predict that $\Delta(P - E)$ should vary similarly to $P - E$ (3). That is to say, wet regions should get wetter and dry regions should get drier. This seems to be the case over the Warm Pool, but elsewhere this direct proportionality is not as apparent.

During the past two decades, the hydrologic parameters E , P , and V exhibited similar responses to the two El Niños (apart from a 6-month lag), similar magnitudes of interannual variability (1.0 to 1.3%), and similar decadal trends (1.2 to $1.4\% \text{ decade}^{-1}$). Earth's surface warmed by $0.2 \text{ K decade}^{-1}$ during this period, and hence the observed changes in E and P suggest an acceleration in the hydrologic cycle of about $6\% \text{ K}^{-1}$, close to the C-C value. In addition, ocean winds exhibited a small increase of $1.0\% \text{ decade}^{-1}$. There is no evidence in the observations that radiative forcing in the troposphere is inhibiting the variations in E , P , and W . Rather, E and P seem to simply vary in unison with the total atmospheric water content.

The reason for the discrepancy between the observational data and the GCMs is not clear. One possible explanation is that two decades is too short of a time period, and thus we see internal climate variability that masks the limiting effects of radiative forcing. However, we would argue that although two decades may be too short

for extrapolating trends, it may indeed be long enough to indicate that the observed scaling relations will continue on a longer time scale. Another possible explanation is that there are errors in the satellite retrievals, but the consistency among the independent retrievals and validation of the winds with other data sets suggests otherwise. Lastly, there is the possibility that the climate models have in common a compensating error in characterizing the radiative balance for the troposphere and Earth's surface. For example, variations in modeling cloud radiative forcing at the surface can have a relatively large effect on the precipitation response (4), whereas the temperature response is more driven by how clouds affect the radiation at the top of the troposphere.

The difference between a subdued increase in rainfall and a C-C increase has enormous impact, with respect to the consequences of global warming. Can the total water in the atmosphere increase by 15% with CO_2 doubling but precipitation only increase by 4% (1)? Will warming really bring a decrease in global winds? The observations reported here suggest otherwise, but clearly these questions are far from being settled.

References and Notes

1. M. R. Allen, W. J. Ingram, *Nature* **419**, 224 (2002).
2. J. F. B. Mitchell, C. A. Wilson, W. M. Cunningham, Q. J. R. *Meteorol. Soc.* **113**, 293 (1987).
3. I. M. Held, B. J. Soden, *J. Clim.* **19**, 5686 (2006).
4. C. Covey *et al.*, *Global Planet. Change* **37**, 103 (2003).
5. F. J. Wentz, M. Schabel, *Nature* **403**, 414 (2000).
6. K. E. Trenberth, J. Fasullo, L. Smith, *Clim. Dyn.* **24**, 741 (2005).
7. G. A. Vecchi *et al.*, *Nature* **441**, 73 (2006).
8. See supporting material on Science Online.
9. F. J. Wentz, *J. Geophys. Res.* **102**, 8703 (1997).
10. T. M. Smith, R. W. Reynolds, *J. Clim.* **18**, 2021 (2005).
11. Data are posted at www.ncdc.noaa.gov/oa/climate/research/gchcn/gchcngrid.html.
12. C. A. Mears, F. J. Wentz, *Science* **309**, 1548 (2005); published online 11 August 2005 (10.1126/science.1114772).
13. G. A. Meehl *et al.*, *Science* **307**, 1769 (2005).
14. R. F. Adler *et al.*, *J. Hydrometeorol.* **4**, 1147 (2003).
15. The satellite-gauge combined precipitation product V2 was downloaded from ftp://precip.gsfc.nasa.gov/pub/gpcp-v2/psg/.
16. J. P. Peixoto, A. H. Oort, in *Physics of Climate* (Springer, New York, 1992), pp. 170–172, 228–237.
17. W. D. Collins *et al.*, *NCAR Technical Note TN-464+STR* (National Center for Atmospheric Research, Boulder, CO, 2004).
18. J. W. Hurrell, Y. Kushnir, G. Ottersen, M. Visbeck, Eds., *The North Atlantic Oscillation: Climate Significance and Environmental Impact* (Geophysical Monograph Series, American Geophysical Union, Washington, DC, 2003), pp. 1–35.
19. W. L. Gates *et al.*, *Bull. Am. Meteorol. Soc.* **73**, 1962 (1998).
20. The more recent AMIP-II simulations were obtained from www-pcmdi.llnl.gov/projects/amiip.
21. B. J. Soden, *J. Clim.* **13**, 538 (2000).
22. This work was supported by NASA's Earth Science Division.

Supporting Online Material

www.sciencemag.org/cgi/content/full/1140746/DC1

Materials and Methods

SOM Text

Fig. S1

References

2 February 2007; accepted 21 May 2007

Published online 31 May 2007;

10.1126/science.1140746

Include this information when citing this paper.

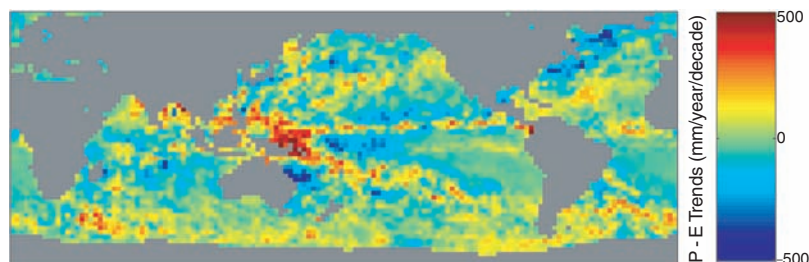


Fig. 3. Trends in satellite-derived $P - E$ for the period July 1987 through August 2006. The largest change was over the warm pool in the western Pacific: a wet area that became wetter.

Table 1. Statistics on the variation of global evaporation, global precipitation, and over-ocean water vapor for the period July 1987 through August 2006. The error bars on the trends are given at the 95% confidence level. The values in parentheses are in terms of percentage change, rather than absolute change.

Parameter	Mean	Standard deviation	Trend
Evaporation	961 mm year^{-1}	$10.1 \text{ mm year}^{-1}$ (1.1%)	$12.6 \pm 4.8 \text{ mm year}^{-1} \text{ decade}^{-1}$ ($1.3 \pm 0.5\% \text{ decade}^{-1}$)
Precipitation	950 mm year^{-1}	$12.7 \text{ mm year}^{-1}$ (1.3%)	$13.2 \pm 4.8 \text{ mm year}^{-1} \text{ decade}^{-1}$ ($1.4 \pm 0.5\% \text{ decade}^{-1}$)
Total water	28.5 mm	0.292 mm (1.0%)	$0.354 \pm 0.114 \text{ mm decade}^{-1}$ ($1.2 \pm 0.4\% \text{ decade}^{-1}$)